Photoelectron microscopy study of the intercalation process in the Cs/4H_b–TaS_2 system

2003 J. Phys.: Condens. Matter 15 5231

(http://iopscience.iop.org/0953-8984/15/30/305)

INSTITUTE OF PHYSICS PUBLISHING JOURNAL OF PHYSICS: CONDENSED MATTER

J. Phys.: Condens. Matter **15** (2003) 5231–5242 PII: S0953-8984(03)60548-5

Photoelectron microscopy study of the intercalation process in the Cs/4H_b–TaS_2 system

S E Stoltz[1] **and H I Starnberg**

Department of Physics, Göteborg University and Chalmers University of Technology, SE-412 96 Göteborg, Sweden

E-mail: stoltz@fy.chalmers.se

Received 6 March 2003
Published 18 July 2003
Online at stacks.iop.org/JPhysCM/15/5231

Abstract

Photoelectron microscopy has been used to study the intercalation process of Cs deposited on a 4H_b–TaS_2 surface. The high spatial resolution of the photoelectron microscope facilitated accurate measurements of spectra from single domains, in contrast to ordinary photoelectron spectroscopy which averages over different domains. Shifts in the Ta 4f core levels were used to identify surface domains with different termination layers. Shifts in the Cs 4d core levels were used to monitor surface absorption and intercalation of Cs. Intercalation was found to occur mainly from step edges, and through defects in domains with octahedrally coordinated termination layers, while Cs deposited in domains with trigonal prismatic termination layers remained on the surface to a larger extent. The observed behaviour is consistent with the charge transfer between the layers in the 4H_b polytype.

(Some figures in this article are in colour only in the electronic version)

1. Introduction

The layered transition metal dichalcogenides (TMDCs) are a group of highly anisotropic materials which exhibit a large number of interesting phenomena [1]. One of these is the possibility to modify the electronic structure of these solids by intercalation with atoms, or small molecules, between the layers [2, 3]. In particular, alkali metals have been used as intercalants, largely because the alkali/TMDC systems are model systems of fundamental interest but also because intercalation in most of these systems is conveniently achieved *in situ* by alkali deposition on clean TMDC surfaces [4].

The formula unit for the TMDCs is TX_2 where T is a transition metal and X stands for S, Se or Te. Each layer consists of a hexagonal sheet of transition metal, which is sandwiched between two hexagonal chalcogen sheets. In the 1T structure, the coordination of the transition

[1] Author to whom any correspondence should be addressed.

0953-8984/03/305231+12$30.00

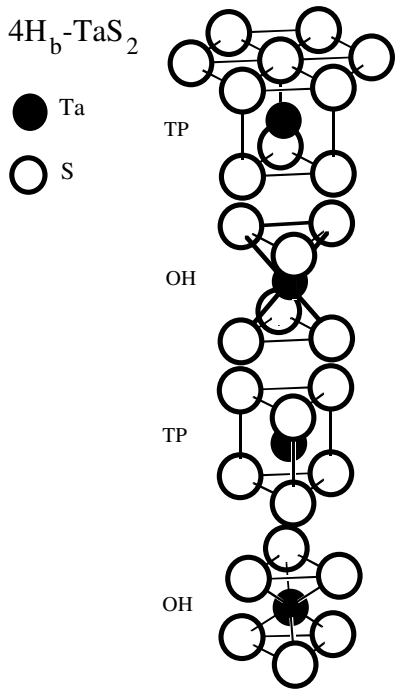

Figure 1. The crystallographic structure of $4H_b$–TaS_2. Layers with TP and OH coordination of the Ta atoms are marked TP and OH, respectively.

metal atoms by the chalcogen atoms is octahedral (OH), while in the 2H structure it is trigonal prismatic (TP). The more complicated $4H_b$ structure, shown in figure 1, is a combination with alternating layers of OH and TP type, and a unit cell which is four layers thick.

The present study is concerned with the behaviour of Cs deposited on clean surfaces of $4H_b$–TaS_2. Since the interlayer interactions are relatively weak, this compound shows properties resembling both 1T–TaS_2 and 2H–TaS_2. An example of this is the existence within the OH layers of a charge density wave (CDW), which is very similar to the one found in the 1T polytype [5]. When $4H_b$–TaS_2 crystals are cleaved, the obtained surfaces exhibit different domains terminated by OH and TP layers, respectively. In conventional photoelectron spectroscopy (PES), the light spot is usually larger than these domains, and the obtained spectra represent an average of the different domains [6]. We have instead used a photoelectron microscope (PEM) with a very small light spot, enabling measurement of spectra from single domains with only one kind of termination layer. In another mode, the PEM can be used to image the distribution of particular atomic species on the surface. This is achieved by detecting photoelectrons from characteristic core levels while the spot is scanned across the sample. As the binding energies of the Ta 4f levels are slightly different for TP and OH terminated domains, these can be directly observed in the imaging mode. Similarly, binding energy differences for the Cs 4d levels allowed us to obtain direct images of both adsorbed and intercalated Cs during the intercalation process. An important objective achieved in this study is to demonstrate how the PEM, through its combination of spatially resolved spectroscopy and element specific imaging, is able to provide detailed information about intercalation of inhomogeneous systems.

2. Experimental details

All core level spectra and images were measured at the undulator based beamline 31 at the MAX-lab synchrotron radiation facility in Lund, Sweden [7]. The beamline comprises a plane-grating monochromator with a Kirkpatrick–Baez objective and a ring-shaped ellipsoidal mirror, which focuses the light onto a small spot (a few microns across) on the sample. The photoelectrons are detected after passing through a conventional hemispherical energy analyser. The PEM is used for spatially resolved PES and for surface imaging by detection of energy-filtered photoelectrons while scanning the sample.

Cs was deposited *in situ* from a carefully outgassed SAES getter source by resistive heating. The Cs source was operated at a current of 5.0 A, and the total sequence of Cs depositions was 1.5, 1.5, 2, 2 × 2, 4 × 2, 8 × 2 and 20 min. No shutter was used, but during the first minute of a deposition the source is warming up and the Cs emission is insignificant. Therefore, the effective accumulated deposition times were 0.5, 1, 2, 4, 8, 16 and 35 min. During the Cs depositions the pressure in the preparation chamber increased from $\sim 5 \times 10^{-10}$ Torr to a maximum of 1.3×10^{-9} Torr. Otherwise the pressure was in the 10^{-10} Torr range, in both preparation and microscope chambers.

The 4H_b–TaS_2 crystal was attached to the sample holder by silver-filled epoxy resin and transferred into the UHV system, where a clean (0001) surface was obtained by cleavage. All measurements where performed at room temperature, in one single experimental run. Additional measurements on other 4H_b–TaS_2 crystals confirmed that the results were reproducible. All results in this study were obtained using a photon energy of 115.3 eV.

3. Results and discussion

3.1. Core levels

Figure 2 shows Ta 4f core level spectra recorded from two reference positions on the surface, one situated in a TP terminated domain and the other in an OH terminated domain (recognized as described below). We have no spectra recorded from these positions prior to the Cs depositions, as they were not selected until after the first Cs deposition. The spectra recorded after the first Cs deposition are still representative for un-intercalated 4H_b–TaS_2, however, as this deposition was too small to cause intercalation. More details of the reference positions are given in section 3.2. The Ta 4f spectra in figure 2 are normalized to the same peak height. However, we observed that the emission decreased with Cs deposition.

Figure 2(a) shows Ta 4f spectra recorded from the reference TP position; they exhibit shoulders typical of TP coordinated layers. The shoulders originate from excitations in the narrow conduction band of the TP layers [6, 8, 9]. The full curve is the spectrum obtained after the first Cs deposition, and it is characteristic for the un-intercalated TP domain. Through additional measurements from other TP positions we have verified that the only significant effect of the first Cs deposition was a small shift ($\sim$0.2 eV) of the Ta 4f peaks towards higher kinetic energy. The dashed curve is the spectrum obtained after the sixth Cs deposition, and represents the intercalated TP domain. The most notable effect of the intercalation is a noticeable increase in the intensities of the Ta 4f shoulders. This is most likely due to changes in the conduction band screening, caused by charge transfer from intercalated Cs.

Figure 2(b) shows the corresponding Ta 4f spectra from the reference OH position. Measurements on other samples confirm that no visible energy shifts (no visible changes at all) appear on OH domains after the first Cs deposition. This is consistent with the very low concentration of Cs on OH domains. We discuss this in more detail in section 3.2.

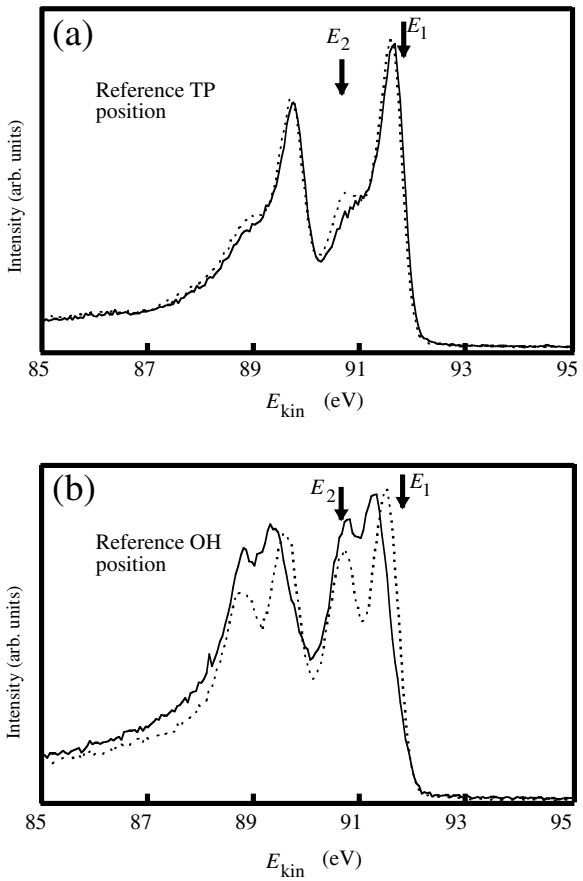

Figure 2. Ta 4f core level spectra from $4H_b$–TaS_2 obtained with $h\nu = 115.3$ eV. The spectra in (a) are from the reference TP position and the spectra in (b) are from the reference OH position. The solid curve spectra are recorded after the first Cs deposition (before intercalation), and the dashed curve spectra after the sixth Cs deposition (after intercalation). The arrows show the kinetic energies used for imaging of TP (E_1) and OH (E_2) domains.

The $\sqrt{13} \times \sqrt{13}$ CDW [5, 6], with the Ta atoms in three inequivalent positions of ratio 6:6:1, splits both spin–orbit components further into two peaks (as the hypothetical third peak is too weak to be discernible). The CDW is formed by the Ta 5d electrons and is localized in the Ta sheet of the OH layer. Therefore, it mainly affects the Ta core levels. The Ta 4f spectrum after intercalation (dashed curve) shows an increased CDW splitting, mainly from an upward shift of the high E_{kin} CDW components. Similar increases in the CDW splitting of Ta 4f levels have previously been observed for 1T–TaS_2 and 1T–$TaSe_2$, and are caused by intercalation-induced changes in the CDW amplitude and periodicity [10–13].

Figure 3 shows how the Ta 4f peaks shifted in the course of repeated Cs depositions. Clearly, the CDW splitting increased abruptly after the fifth Cs deposition (corresponding to a total effective deposition time of 8 min). We attribute this abrupt change to the passing of an intercalation front across the reference OH position. This interpretation is further supported by the images presented in section 3.2. The observation of an abrupt change in the CDW splitting contrasts with previous studies of the similar Cs/1T–$TaSe_2$ system, where the splitting increased gradually with the amount of Cs [11, 12]. It is possible that the earlier reported

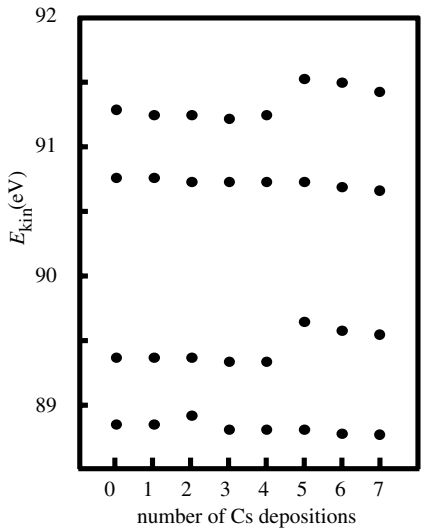

Figure 3. Peak positions in the Ta 4f spectra from the reference OH position as a function of Cs depositions. The sudden increase in the CDW splitting after the fifth Cs deposition is clearly visible.

gradual shift originated from a superposition of two peaks at slightly different energies, one from Ta 4f in an un-intercalated area and one from Ta 4f in a nearby intercalated area. During the intercalation process the relative size of these areas changes gradually, and the resulting superposition in the PES spectrum may then appear as one gradually shifting peak. However, there remains a possibility that the intercalation process in the 1T system is more gradual, without the sharp intercalation fronts our present data suggest for the Cs/4H$_b$–TaS$_2$ system. Clearly there is a need for more studies, by methods capable of high spatial resolution, to conclude whether the intercalation process is fundamentally different for 1T and 4H$_b$ systems.

Some selected Cs 4d core level spectra are shown in figure 4. The spectra in figure 4(a) were recorded from the TP reference position and the spectra in figure 4(b) were recorded from the OH reference position. The full and dashed curves are spectra recorded after the first and sixth Cs depositions respectively. In general, each Cs 4d spectrum is a superposition of two Cs 4d spin–orbit doublets, with a relative shift that depends on the termination layer. It is well established from studies of similar systems that the doublet of highest kinetic energy is due to intercalated Cs, while the other doublet corresponds to Cs adsorbed on the surface [14–18]. Peaks in figure 4 associated with surface and intercalated Cs have been marked S and I respectively. In the following we denote surface and intercalated Cs by Cs(S) and Cs(I) respectively. The Cs spectra from the reference TP position were normalized with respect to the saturation level of Cs(S), which was already reached after the first Cs deposition. The Cs spectra from the reference OH position were normalized with respect to the background emission on the high kinetic energy side. This probably overestimated somewhat the intensity after the first Cs deposition.

It is notable that the Cs(I) peaks appear at the same energies for both kinds of domain, while Cs(S) peaks are differently shifted depending on the termination layer. A TP termination layer gives a relative shift of $\sim$1 eV, while an OH termination layer gives a shift of $\sim$1.5 eV.

A special property of the 4H$_b$ polytype, in contrast to the 1T and 2H polytypes, is that there is charge transfer between the layers [6], making the TP and OH layers negatively and

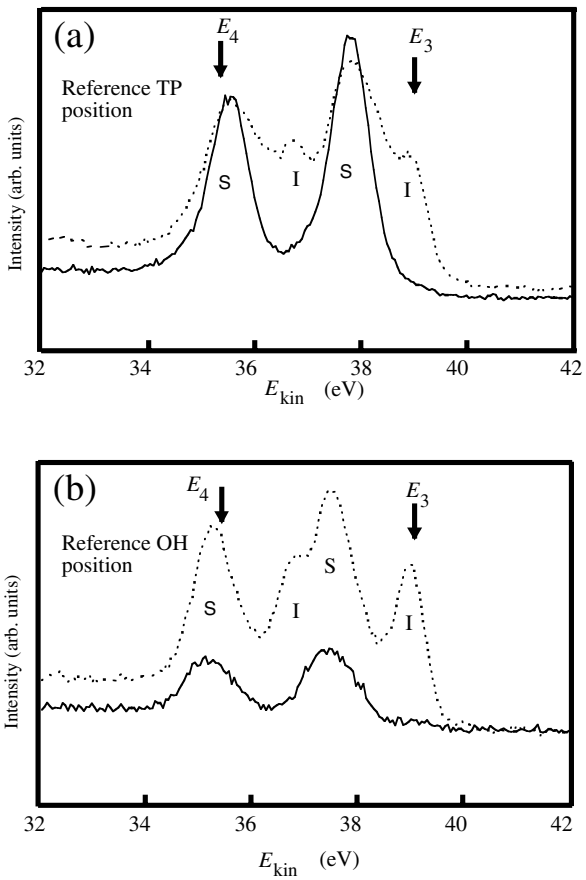

Figure 4. Cs 4d core level spectra from $4H_b$–TaS_2 obtained with $h\nu = 115.3$ eV. The spectra in (a) are from the reference TP position, and the spectra in (b) are from the reference OH position. The solid curve spectra are recorded after the first Cs deposition (before intercalation), and the dashed curve spectra after the sixth Cs deposition (after intercalation). Peaks originating from intercalated and surface Cs are marked I and S respectively. The arrows show the kinetic energies used for imaging of intercalated Cs (E_3) and Cs on the surface (E_4).

positively charged respectively. One manifestation of this charge transfer is that the Ta 4f peaks from a TP domain, on average, appear at higher kinetic energy than the Ta 4f peaks from an OH domain. Also the energy differences between Cs(S) photoelectrons from TP and OH domains, respectively, can be attributed to the electrostatic charging of the layers. The absence of any termination-dependent shifts for the Cs(I) peaks is not surprising, because Cs(I) is always sandwiched between one OH and one TP layer, irrespective of surface termination. The energy differences we observed are thus consistent with the charge transfer between the layers, and confirm the quality of the $4H_b$ crystal. If the sample instead had been a domain structure of 1T and 2H polytypes we would not have observed these characteristic electrostatic core level shifts.

3.2. Images

The PEM was used to image a 620 μm × 120 μm stripe of the surface. Each stripe is actually a composite of six 120 μm × 120 μm square images. The 20 μm overlap between the squares

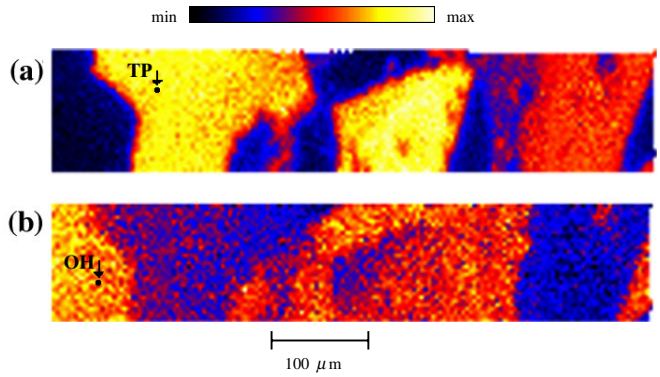

Figure 5. PEM images of 4H$_b$–TaS$_2$ highlighting areas with (a) TP, and (b) OH termination. The size of the images are 620 × 120 μm. The reference TP and OH positions are marked as black dots in (a) and (b), respectively. The intensity scale is shown above the images.

was used to calculate relative normalization factors by comparing the intensities in the overlap region.

By setting the analyser to suitable kinetic energies in the Ta 4f range, we were able to highlight TP and OH terminated areas separately. Analogously, by selecting kinetic energies in the Cs 4d range, we obtained images of how Cs(I) and Cs(S) were distributed on the surface stripe. The following kinetic energies were used for the various imaging purposes: for TP domains $E_1 = 91.7$ eV; for OH domains $E_2 = 90.65$ eV, Cs(I) $E_3 = 39.1$ eV and Cs(S) $E_4 = 35.4$ eV. These energies are indicated by arrows in figures 2 and 4.

Figure 5 shows images highlighting (a) TP and (b) OH domains before the Cs depositions. These images are complementary for most of the depicted area, which indicates a high-quality surface. The reference TP and OH positions are marked in the figure. It should be noted, however, that the signals used for recording the OH and TP images are somewhat mixed. In particular, this affects the OH image, because the spectral peak used coincides with the shoulder in the TP domain spectrum. An area with a strong signal in the TP image will therefore also generate a false intensity in the OH image. To avoid this problem we have reconstructed the images by making linear combinations of the measured TP and OH images. If TP$_0$ and OH$_0$ are hypothetical domain-specific signals, the measured TP and OH signals are related to these through:

$$\mathrm{TP} = a_{11}\mathrm{TP}_0 + a_{12}\mathrm{OH}_0 \tag{1}$$

$$\mathrm{OH} = a_{21}\mathrm{TP}_0 + a_{22}\mathrm{OH}_0. \tag{2}$$

The diagonal matrix elements (a_{11} and a_{22}) were chosen to be unity (1), and the values of the off-diagonal elements (a_{12} and a_{21}) were determined from the core level spectra. The value of a_{12} is obtained as the ratio between the intensities at the energies E_1 and E_2 in the OH domain spectrum (figure 2(b), full curve). In the same way, a_{21} is obtained as the ratio between the intensities at the energies E_2 and E_1 in the TP domain spectrum (figure 2(a), full curve). The values of these two elements are $a_{12} = 0.37$ and $a_{21} = 0.42$.

The linear combination for the reconstructed images is obtained by inverting the matrix:

$$\mathrm{TP}_0 = b_{11}\mathrm{TP} + b_{12}\mathrm{OH} \tag{3}$$

$$\mathrm{OH}_0 = b_{21}\mathrm{TP} + b_{22}\mathrm{OH} \tag{4}$$

where $b_{11} = b_{22} = 1.184$, $b_{12} = -0.44$ and $b_{21} = -0.49$. In the reconstructed images, the intensity should drop to zero in areas where the termination is not of the selected kind.

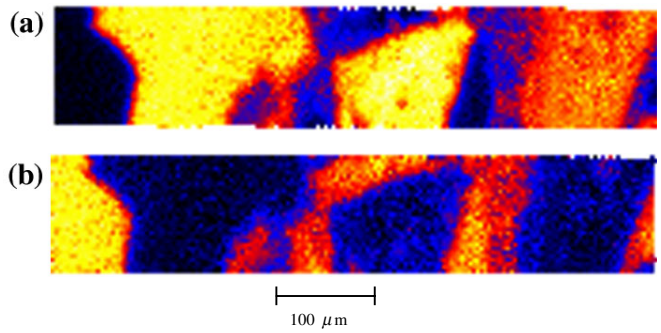

Figure 6. Reconstructed TP and OH images, obtained from linear combinations of the original TP and OH images in figure 5. TP domains are highlighted in (a) and OH domains in (b).

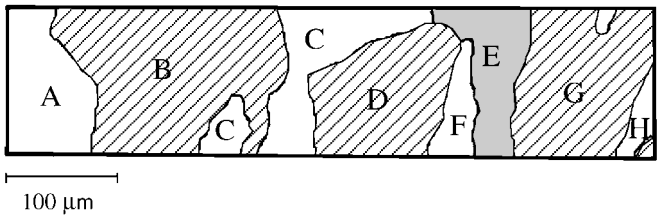

Figure 7. Drawing of the studied stripe, where TP domains are cross-hatched, OH domains are white and an area of unclear designation is grey. The termination layers of the different areas are probably stacked as follows: $\frac{A}{B}$, $\frac{B}{C}$, $\frac{D}{C}$, $\frac{F}{D}$ and $\frac{G}{H}$. Between the areas F and G is an area E without a well-defined termination layer.

However, because of the noise, we instead obtained intensity values centred around zero. As negative values are unphysical, we used the absolute values when drawing the images. The reconstructed images are shown in figure 6, and are found to be complementary with exception for one area. From the images in figure 6, we are able to accurate identify the surface regions with TP and OH termination layers, respectively, but not their stacking order. The result is shown in figure 7 as a map of the studied stripe. The different areas are labelled with letters A–H, and their termination layers are indicated.

The distributions of Cs(S) and Cs(I) were imaged after each Cs deposition. These images are shown in figure 8 for Cs(S) and in figure 9 for Cs(I). Here we are able to follow the successive Cs filling of the sample. In each of these images, white represents the point with the highest intensity, and black represents the point with the lowest intensity. Some areas were already filled to their saturation level after the first Cs deposition. There was therefore no need for further normalization as long as at least one point in the image remained almost free of Cs. This is the case in all but the last images, where we instead put in one artificial low-intensity point (outside the image) to preserve the scale. The intensity of this imaginary point was chosen by use of the constant ratio intensity between Cs-saturated and Cs-free areas. In the Cs images there was no need for reconstruction of the images, as the peaks used to depict Cs(S) and Cs(I) do not interfere significantly (see spectra in figure 4).

After Cs deposition, one may find the stacking order by considering the motion of the intercalation fronts in the Cs(I) images of figure 9. The intercalation fronts typically begin at step edges, and it is logical to assume that Cs moves under the layer which is on top. For example, the intercalation front at the sharp edge $\sim$70 μm from the left edge of the image

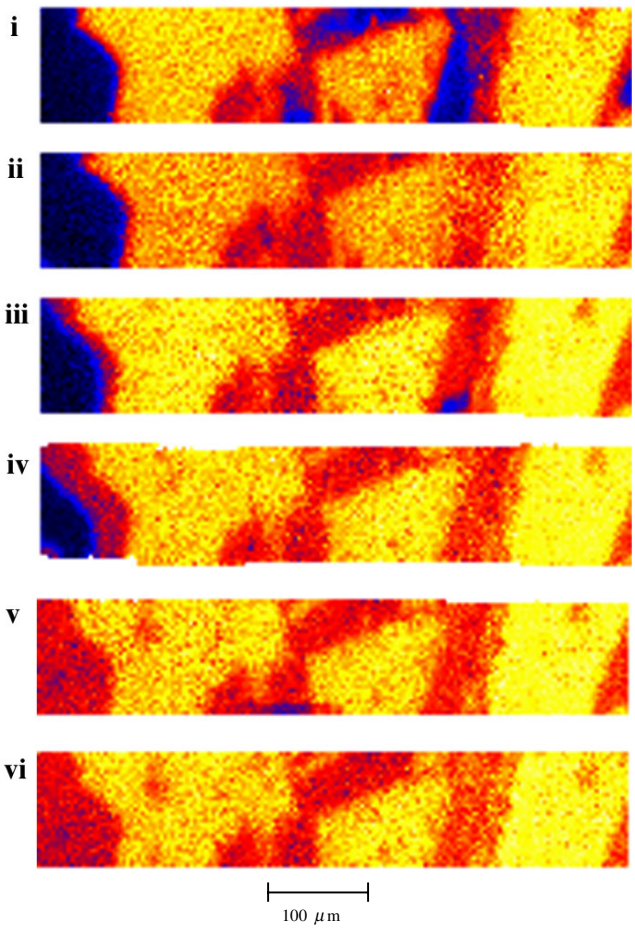

Figure 8. PEM images of the same stripe as in figure 5, but highlighting areas with surface Cs as more Cs is successively deposed. The effective deposition times were (from the top): 0.5, 1, 2, 4, 8 and 16 min.

moves to the left. Therefore, using the domain labels of figure 7, the OH layer A is on top of the TP layer B. We denote this stacking order by $\frac{A}{B}$. By considering other intercalation fronts as well, we were able to work out the stacking in the whole depicted area. From a larger image we know that the both areas marked C are connected. The termination layer in area C is below the termination layer in both area B and area D ($\frac{B}{C}$, $\frac{D}{C}$). Similarly we conclude that $\frac{G}{H}$ and probably $\frac{F}{D}$. Between the areas F and G we have an area E without a well-defined termination layer.

A difference between the OH terminated areas A and C is that intercalation occurs immediately over the whole area C, while area A is intercalated only from the borders. The reason for this difference is probably that the termination layer in area C has a large number of defects, while area A has a more perfect termination layer. We note that an intercalation front appears on the left side of area G, but clearly to the right of the border with area E. This indicates that area G actually comprises two domains, separated by a double step (not visible on the images of the pure crystal), with the right domain being on top. In principle, the steps denoted as single or double could actually be any odd or even number of layers respectively.

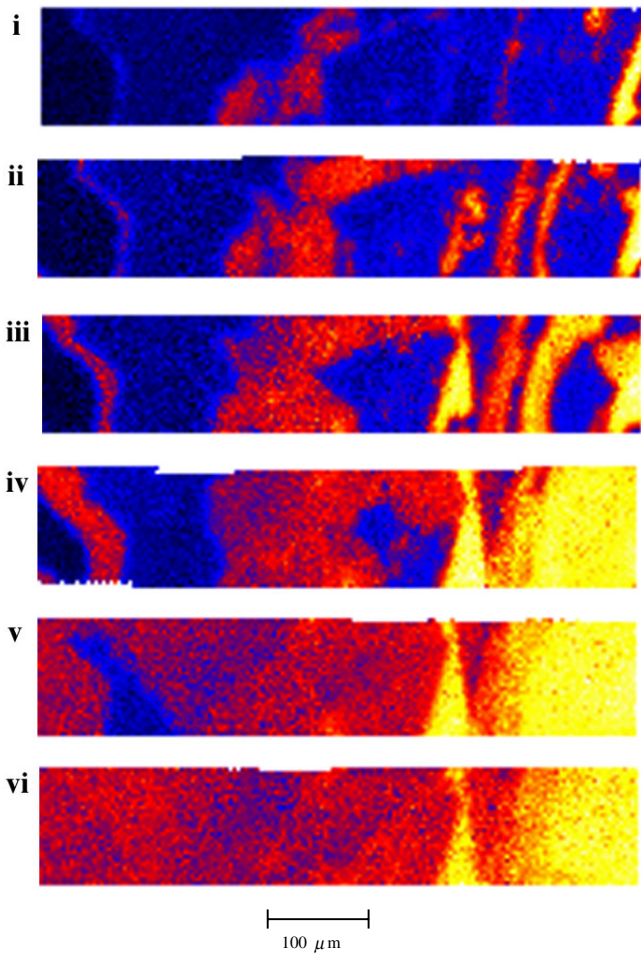

Figure 9. PEM images of the same stripe as in figure 5, but highlighting areas with intercalated Cs as more Cs is successively deposed. The effective deposition times were (from the top): 0.5, 1, 2, 4, 8 and 16 min.

However, from the large number of odd step borders (compared with the small number of even step borders) and the mirror-like surface of the sample, we believe that the steps are in most cases one layer, and that two-layer steps are the second most common type.

An effect of the charge transfer between the layers is the behaviour of the Cs(S). During adsorption, each Cs atom leaves an electron and becomes a Cs^+ ion. Therefore, Cs(S) is attracted to domains with a negatively charged TP termination layer, and already reaches the saturation level after the first Cs deposition.

For an area with an OH termination layer the amount of Cs(S) is very low after the first Cs depositions, but increases step-wise after intercalation has occurred. This is consistent with a decrease in the charge exchange between the layers, caused by the increased layer separation due to intercalation. The abundance of Cs(S) is always higher for areas with TP termination, however.

After having reached a saturation level of Cs(I), we still found some areas with a more intense Cs(I) signal. These areas are both OH and TP terminated (e.g. F and G). Also, different

domains (of the same type) in the TP and OH images are not equally intense. The more intense Cs(I) signal comes in particular from domains with a weaker Ta 4f signal from the host layers. The reason for these intensity variations is not clear, but may be associated with variations in the quality of the crystal. It is notable that the largest Cs(I) signals are found in the rightmost part of the imaged stripe, where the step density is higher and the intercalation patterns are more irregular. It therefore seems that the middle and leftmost parts are more representative of high-quality surfaces of $4H_b$–TaS_2. Here the intercalation after the sixth Cs deposition is very homogeneous, irrespective of surface termination.

4. Conclusions

We have demonstrated that PEM is able to reveal new interesting aspects of the intercalation process in layered TMDC crystals by offering a combination of images and spatially resolved core level spectra.

The obtained results verify that cleaved $4H_b$–TaS_2 surfaces have complementary domains of TP and OH termination respectively. Domain sizes are typically of the order $\sim$0.1 mm. Using the spatial resolution of the PEM we were able to obtain accurate core level spectra separately from TP and OH domains.

The Cs intercalation was found to occur as fronts beginning at step edges, or through distributed defects. The adsorption of Cs on the surface preferably took place on TP terminated domains, which can be attributed to the electron transfer from OH to TP layers in the $4H_b$ polytype. Essentially the same saturation level of intercalated Cs was reached in the different domains, despite differences in the intercalation process. Anomalously high levels of intercalated Cs were found in some domains, however, presumably due to a higher density of defects.

It is important to point out that the intercalation process in 1T and 2H polytypes of TMDCs could be distinctly different, as they lack the charge transfer between layers, which was found to have profound effects on both adsorption and intercalation.

Acknowledgments

We want to thank F Lévy for providing the $4H_b$–TaS_2 samples and the staff at MAX-lab, in particular A Zakharov, for valuable assistance. This work was supported by the Swedish Research Council.

References

[1] Wilson J A and Yoffe A D 1969 *Adv. Phys.* **18** 193
[2] Lévy F A (ed) 1979 *Intercalated Layered Materials* (Dordrecht: Reidel)
[3] Friend R H and Yoffe A D 1987 *Adv. Phys.* **36** 1
[4] Starnberg H I, Brauer H E and Hughes H P 2000 *Electron Spectroscopies Applied to Low-Dimensional Materials* ed H P Hughes and H I Starnberg (Dordrecht: Kluwer) p 41
[5] Ekvall I, Kim J and Olin H 1997 *Phys. Rev.* B **55** 6758
[6] Hughes H and Scarfe J 1996 *J. Phys.: Condens. Matter* **8** 1457–73
[7] Johansson U 1997 *PhD Thesis* Lund University
[8] Hughes H and Scarfe J 1996 *J. Phys.: Condens. Matter* **8** 1421–38
[9] Hughes H and Scarfe J 1996 *J. Phys.: Condens. Matter* **8** 1439–55
[10] Pettenkofer C and Jaegermann W 1994 *Phys. Rev.* B **50** 8816
[11] Crawack H J, Tomm Y and Pettenkofer C 2000 *Surf. Sci.* **465** 301
[12] Crawack H J and Pettenkofer C 2001 *Solid State Commun.* **118** 325
[13] Stoltz S E, Starnberg H I and Holleboom L J 2003 *Phys. Rev.* B **67** 125107

[14] Pettenkofer C, Jaegermann W, Schellenberger A, Holub-Krappe E, Papageorgopoulos C A, Kamaratos M and Papageorgopoulos A 1992 *Solid State Commun.* **84** 921
[15] Brauer H E, Starnberg H I, Holleboom L J and Hughes H P 1995 *Surf. Sci.* **331–333** 419
[16] Brauer H E, Starnberg H I, Holleboom L J, Strocov V N and Hughes H P 1998 *Phys. Rev.* B **58** 10031
[17] Brauer H E, Starnberg H I, Holleboom L J, Strocov V N and Hughes H P 1999 *J. Phys.: Condens. Matter* **11** 8957
[18] Brauer H E, Starnberg H I, Holleboom L J, Hughes H P and Strocov V N 2001 *J. Phys.: Condens. Matter* **13** 9879